sciendo Acta Marisiensis - Seria Medica 2024;70(2):68-74 DOI: 10.2478/amma-2024-0015

RESEARCH ARTICLE

The effects of pearl oyster shell-derived bone grafts on TNF-alfa levels: An *in vivo* study in *Cavia porcellus*

Sri Oktawati[1], Nurlindah Hamrun[2*], Muthmainnah Muthmainnah[1], Dian Setiawati[1], Andi Sitti Hajrah Yusuf[3]

1. Department of Periodontology, Faculty of Dentistry Hasanuddin University, Makassar, Indonesia
2. Department of Oral Biology, Faculty of Dentistry Hasanuddin University, Makassar, Indonesia
3. Department of Oral and Maxillofacial Surgery, Faculty of Dentistry Hasanuddin University, Makassar, Indonesia

Objective: This study aims to assess the effect of bone graft materials derived from pearl oyster shells on the tumor necrosis factor-alpha (TNF-α) level.
Methods: This research utilized a bone graft containing hydroxyapatite Pinctada maxima (HPM) powder obtained from pearl oyster shells. Material testing was conducted on 30 male guinea pigs aged 8-10 weeks, divided into three groups: the negative control group, the group treated solely with HPM, and the group treated with HPM combined with platelet-rich fibrin (PRF). Each treatment group was observed for 7 and 14 days. The results were analyzed using One-way ANOVA with a significance level of $p<0.05$.
Results: The findings demonstrated a decrease in the average TNF-α levels across all groups. On observation days 7 and 14, the HPM group exhibited a significant difference compared to the negative control group, indicating reduced TNF-α levels. However, no significant difference was observed when comparing the HPM group with the HPM and PRF groups.
Conclusions: Bone grafts derived from pearl oyster shells possess high levels of hydroxyapatite, and the addition of PRF into the bone graft effectively reduces TNF-α.

Keywords: bone graft, Pinctada maxima, pearl oyster shells, platelet-rich fibrin, TNF-alfa

Received 24 October 2023 / Accepted 3 June 2024

Introduction

Periodontal disease represents a prevalent oral chronic condition characterized by inflammation and destruction of the supporting structures of the teeth, including the alveolar bone and periodontal ligament [1-3]. It initiates as a superficial inflammation of the gingiva and can advance into attachment loss and subsequent destruction of tooth-supporting structures [1,2]. Emerging evidence suggests a complex interplay between periodontal disease and systemic health, with chronic inflammation in the oral cavity potentially contributing to systemic inflammation and the pathogenesis of various systemic diseases [1-3]. Conventional treatments for periodontal disease, like scaling and root planning or open flap debridement, have been considered the gold standard [3]. However, these surgical methods have limited potential in achieving complete periodontal regeneration [2]. Thus, different types of bone grafts have been extensively used to promote bone formation and periodontal regeneration [2].

In medical research, pursuing innovative treatment options that enhance the regenerative potential of bone tissues remains a paramount focus [4,5]. Bone grafts, a popular therapeutic intervention, have promoted bone repair and regeneration [4,5]. Among the myriad of materials utilized for this purpose, pearl oyster shell (Pinctada maxima) has emerged as a promising candidate due to its abundance, biocompatibility, and potential to mimic the natural composition of bone [5,6]. This natural marine biomaterial possesses many advantages, for example, low cost, sophisticated predesign of hierarchical structures and architectures for biorecognition, intrinsic biological functions, the possibility of low-level immunogenicity, low cytotoxicity, and easy safe storage [5,6]. These characteristics collectively contribute to the exceptional potential of Pinctada maxima in developing bone graft materials [5,6}.

Bone remodeling is a gradual and continuous process that relies on the coordinated activity of osteoclasts and osteoblasts [7,8]. The proper cycle of bone remodeling is essential for maintaining bone health [7,8]. The relationship between inflammatory processes and new bone formation has recently gained increasing attention [7,8]. In particular, elevated levels of pro-inflammatory cytokines, such as tumor necrosis factor-alpha (TNF-α), have been implicated in the progression of periodontal disease and associated systemic complications [7,8]. TNF-α is one of the major pro-inflammatory cytokines that traditionally regulates bone homeostasis by stimulating the osteoclast process and inhibiting osteoblast function [4,7]. Emerging evidence suggests a complex interplay between periodontal disease and systemic health, with chronic inflammation in the oral cavity potentially contributing to systemic inflammation and the pathogenesis of various systemic diseases [4,7,8]. Excessive levels of TNF-α can lead to increased bone resorption as it triggers the proliferation and differentiation of osteoclast progenitors, indirectly promoting osteoclast formation [4,9]. The overexpression of TNF-αmay lead to

* Correspondence to: Anca Cighir
E-mail: anca.cighir@umfst.ro

prolonged inflammation, hindering the initiation of bone healing and impairing the regenerative process [4,9,10]. Given the pivotal role of TNF-α in inflammation and tissue destruction, interventions aimed at modulating its levels hold promise for managing periodontal disease and its systemic consequences [4,9,10]. In light of this background, this study aims to elucidate the effect of bone graft materials derived from pearl oyster shells on the level of TNF-α. The findings from this research hold the potential to pave the way for the development of advanced bone graft materials that not only promote osteogenesis but also alleviate inflammatory responses, thereby expediting the overall healing process.

Methods

Preparation of hydroxyapatite Pinctada maxima (HPM) bone graft

Pearl shells from Pinctada maxima were sourced from the Pangkep Islands in South Sulawesi, Indonesia. Pinctada maxima were supplied raw and prepared as specified in the following procedure. First, the shells were cleaned by brushing under flowing water and sun drying. Subsequently, the cleaned shells were fragmented into smaller pieces and subjected to a 2-hour furnace treatment. The resulting samples were then crushed using a metal mortar and pestle, and the obtained material was filtered through a test sieve (100 mesh) to yield Pinctada maxima pearl shell powder.

The precipitation technique was employed to synthesize hydroxyapatite (HAP) from Pinctada maxima shell powder. The shells of Pinctada maxima were subjected to synthesis using H3PO4 compounds under a temperature of 100°C. The solution was allowed to stand for 24 hours to facilitate the formation of HAP deposits. These deposits were subsequently subjected to a calcination process at 800°C. The end product of this synthesis process was HPM powder. The chemical and structural properties of HPM were evaluated through analytical methods of Fourier Transform Infrared (FTIR) analysis.

Animal model

This experiment was approved by the Ethics Committee of the Faculty of Dentistry, Hasanuddin University, Makassar, Indonesia, with approval number 0064/PL.09/KEPK FKG-RSGM UNHAS/2022. All animal procedures were conducted strictly per relevant guidelines and regulations with every effort to minimize animal suffering. Male guinea pigs (*Cavia porcellus*) weighing 250–300 g and aged 2–3 months (n = 30) were used in this experiment. Before the experiment, the *Cavia porcellus* was adapted to a 12-h light/12-h dark cycle and given free access to tap water and standard food for a week. Unhealthy *Cavia porcellus* were excluded if they lost more than 10% of their body weight after a week of adaption.

Guinea pigs received an intramuscular injection of ketamine (50 mg/kg) and xylazine (5 mg/kg), which were mixed and injected with a dose of 1 mg/kg BB in Dexter's femur bone. After shaving and asepsis with 10% povidone-iodine, a 2 cm long horizontal incision using blade no. 15 on soft tissue to reduce bleeding and a full-thickness flap was made. The skin and muscles were lifted with a periosteal elevator where the defect would be made. After the bone tissue was exposed, a defect was made with a round bone bur (5 mm diameter and 1 mm depth). The hole in the femur was randomly treated according to the allocated treatment groups. Group A was treated with a placebo (negative control); in Group B, the defect was treated with an HPM bone graft; in Group C, the defect was treated with an HPM bone graft mixed with platelet-rich fibrin (PRF). The amount of material introduced was approximately 7.0 mg.

After the surgical procedure, the suture was performed with absorbable suture (Vicryl 5.0) on the muscles and silk suture on the skin, with interrupted suture technique, and given antibiotics as prophylaxis on the surface of the suture area. For post-surgical medication, the guinea pig was given dexamethasone 0.6 mg/kg and ampicillin 10 mg/kg. Euthanasia was performed with an ether chamber at 7 and 14 days, in which five animals were sacrificed in each group at a time. The femur was taken through appropriate surgical techniques, and the bone defects were separated. Pieces of the bone block were stored in a 10% formalin solution for 24 hours and then sent to the Microstructure Laboratory for a routine laboratory procedure.

Immunohistochemical testing

Paraffin-embedded bone tissue blocks were sliced into four µm-thick sections using a microtome and deparaffinization with xylene. Subsequently, rehydration was carried out using progressively decreasing concentrations of ethanol. This was followed by rinsing the tissue sections with Phosphate Buffer Saline (PBS) for three sets of five-minute intervals each. The tissue samples were then incubated in DAKO® Buffer Antigen Retrieval solution within a microwave at 94°C for 20 minutes, followed by a cooling period at room temperature for another 20 minutes.

The subsequent steps involved washing the preparations with PBS for three sets of five-minute intervals, then incubating them in Peroxidase Block (Novocastra®) for 20 minutes. Afterward, the preparations were washed again with PBS for three sets of five-minute intervals, then incubated in Protein Block for 20 minutes. Following this, another round of PBS washing was done for three sets of five-minute intervals each. The preparations were then incubated overnight (12-18 hours) with a primary antibody against TNF-α protein at 4°C.

The following day, the preparations were rinsed with PBS for three sets of five-minute intervals each. Then, they were treated with post-primary and post-protein solutions for 45 minutes, followed by incubation with a secondary antibody (Novolink® Horse Radish Peroxidase - HRP) for 60 minutes at room temperature. After this incubation, the

samples were washed with PBS for three sets of five-minute intervals each and counterstained with hematoxylin (Novocastra). Subsequent steps included dehydration using gradually increasing ethanol concentrations, a clarification step using xylene, and mounting. The final step involved air-drying the slide, applying Entellan, and covering it with a coverslip. The prepared slide was then observed under a microscope for analysis.

Image analysis

Each tissue specimen was sectioned to a thickness of 4 micrometers, followed by immunohistochemical analysis to assess the TNF-α levels. After this, a blinded examination was conducted. The evaluation and quantification involved observing the presence of a brown hue within the cytoplasm of osteoblast cells. The calculations were based on a methodology outlined by Soini et al. (1998) and modified according to the specifications of Pizem and Cor (2003), tailored to suit osteoblast cells with TNF-α levels. This quantification was performed across 20 fields of view using a light microscope at a magnification of 1000x (ocular-objective).

Hematoxylin-Eosin (HE) staining was also conducted to provide a structural reference. The immunohistochemical staining was deemed negative if no cells exhibited brown-stained nuclei granules. At the same time, a positive judgment was assigned if granule cells with brown nuclei were observed within the cell nucleus.

Statistical analysis

Numerical information is expressed using mean–standard deviation. The normality of the data was assessed using the Shapiro-Wilk test, while the homogeneity of the data was evaluated using Levene's test. The paired t-test was employed to compare the difference between 7-day and 14-day time points. Data analysis between different groups was conducted using one-way ANOVA, while the Tukey HSD post hoc test was employed to compare data among the three groups. All statistical analyses were performed using the SPSS program (IBM Statistics version 21), and significance was determined for differences with a threshold of $P<0.05$.

Results

Characteristics of HPM graft materials

FTIR analysis data can offer a qualitative prediction of the HAP content in HPM graft materials. This analysis provides valuable insights into sample composition by examining peak locations, intensities, widths, and shapes within the designated wave-number range. Notably, this analysis has revealed the presence of specific functional groups, including OH- (hydroxyl), PO43- (phosphate), and CO32- (carbonate) groups. The recorded data from the analysis indicates the identification of hydroxyl groups at the wave number 3641.73 cm-1, phosphate groups at 563.59 cm-1, 609.53 cm-1, and 1035.81 cm-1, and calcium carbonate groups at 1425.44 cm-1 and 1512.24 cm-1 as shown in Figure 1. The research findings demonstrate an observable increase in crystallization growth attributed to HAP's specific functional group structure. The characteristic infrared spectrum bands strongly suggest the presence of HAP within the tested material compound.

Immunohistochemical analysis

The results of the Shapiro-Wilk normality test indicated that the data exhibited a normal distribution, as evidenced by a mean p-value of 0.546 ($p>0.05$). Furthermore, the homogeneity test for the data yielded a significance level of 0.526 ($p>0.05$). This observation concludes that the TNF-α level variants being compared across all groups on

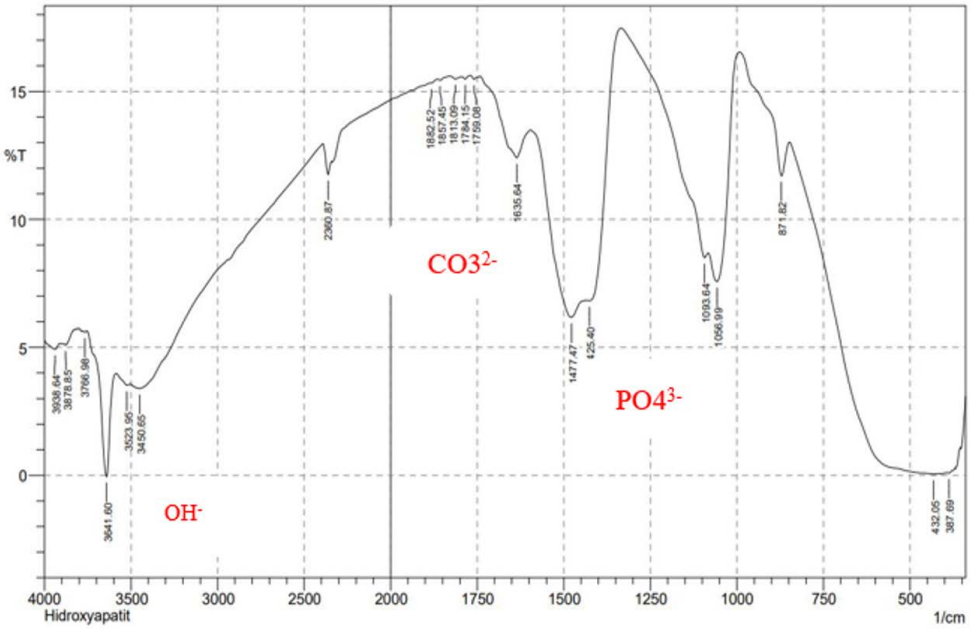

Fig. 1. The FTIR analysis of HPM graft materials highlights the presence of OH-, PO43-, and CO32- functional groups.

the 7th and 14th days possess similarity or homogeneity, thus satisfying the assumption of data homogeneity.

Figure 2 illustrates a descriptive decrease in the mean TNF-α levels across all groups on days 7 and 14. Results indicated a reduction in the mean TNF-α levels across the three treatments on days 7 and 14. In group A, the average TNF-α level on day 7 was 11.4 pg/ml, which decreased to 8.4 pg/ml on day 14. In group B, the average TNF-α level on day 7 was 9.2 pg/ml, which decreased to 5.8 pg/ml on day 14. Likewise, in group C, the average TNF-α level l on day 7 was 7.2 pg/ml, which decreased to 3.4 pg/ml on day 14.

Figure 3 and Figure 4 display immunohistochemical images representing the presence of TNF-α in osteoblast cells on days 7 and 14. In Figure 3, the TNF-α expression on day seven is depicted in a brownish color across all groups, with Group C showing the highest TNF-α expression compared to the other groups. Figure 4 illustrates the TNF-α expression on day 14 in all groups: the control group, the HPM bone graft-only, and the HPM bone graft combined with the PRF. In all groups, TNF-α expression is observable, indicated by the brownish coloration, with the highest level found in the HPM bone graft combined with the PRF group.

Table 1 depicts the immunohistochemical observation rates of TNF-α levels in femur defects based on the observation time for each study group. The ANOVA test yielded significant results only in group C ($p<0.05$). This significance implies a notable difference between the observations made on the 7th and 14th days of the group C.

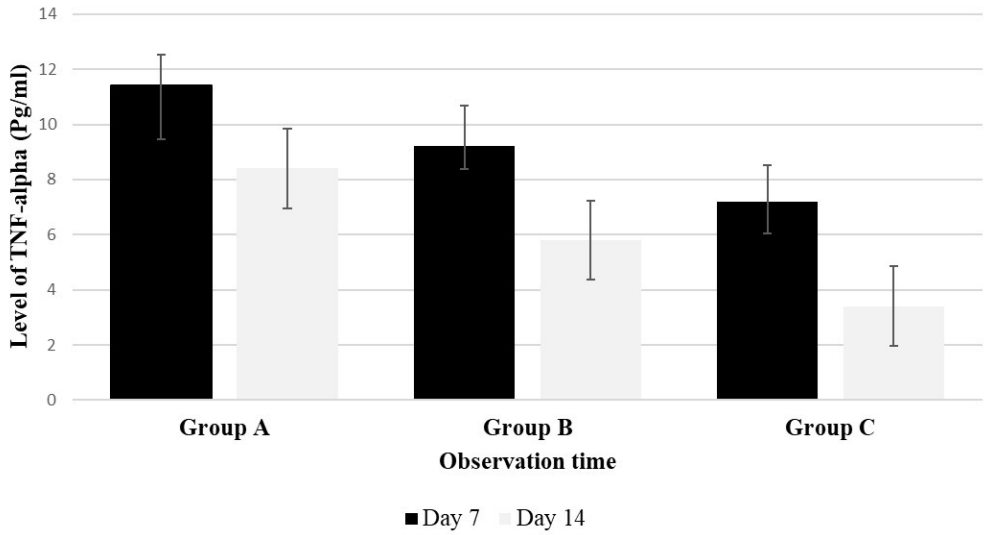

Fig. 2. The average TNF-α levels were observed through immunohistochemistry on the 7th and 14th days. Group A (negative control), Group B (HPM only), and Group C (HPM combined with PRF).

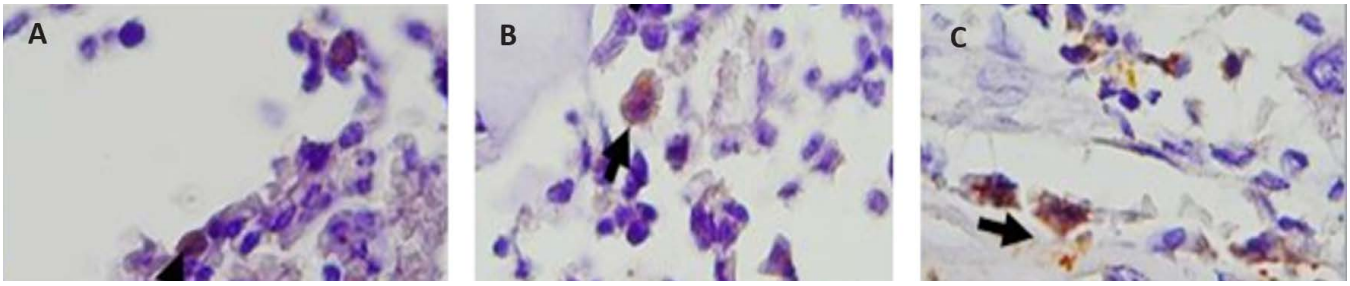

Fig. 3. The TNF-α expression on the 7th day under a light microscope with a 1000x magnification. (A) Group A: negative control, (B) Group B: HPM only, and (C) Group C: HPM combined with PRF; TNF-α level marked in brown (arrowheads).

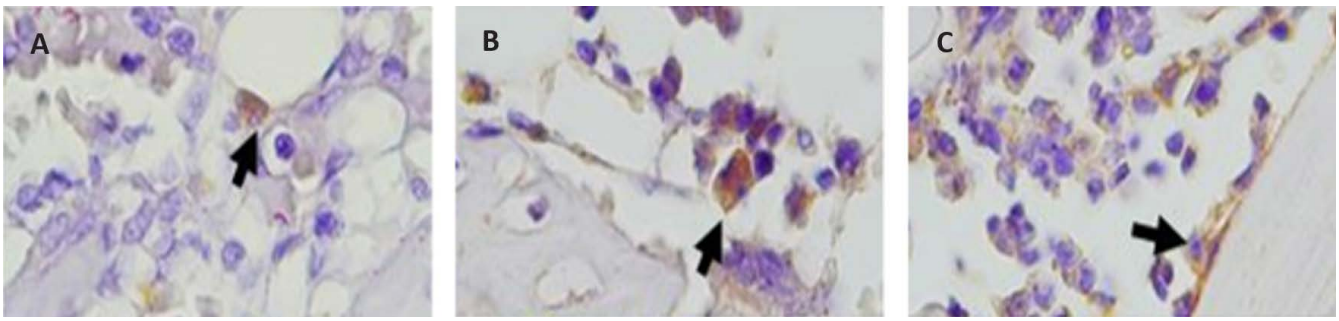

Fig. 4. Expression of TNF-α on the 14th day under a 1000x magnification light microscope. (A) Group A: negative control, (B) Group B: HPM only, and (C) Group C: HPM combined with PRF, TNF-α level marked in brown (arrowheads).

Table I. Comparison of the mean and standard deviation of TNF-α levels in each experimental group.

Group	N	Observation	Mean±SD	p-value
Group A (negative control)	5		11.4±1.14	
Group B (HPM alone)	5	7	9.2±1.483	0.001*
Group C (HPM+PRF)	5		7.2±1.304	
Group A (negative control)	5		8.4±1.949	
Group B (HPM alone)	5	14	5.8±0.837	0.001*
Group C (HPM+PRF	5		3.4±1.140	

*ANOVA test; p<0.05 significant.

In contrast, the p-value was greater than 0.05 for groups A and B, indicating no significant difference between the observations on the 7th and 14th days within these groups. The table illustrates a decline in the average values for the three groups: the negative control, HPM alone, and a combination of HPM with PRF. This decrease signifies a reduction in inflammation over time, suggesting that the addition of PRF has an effect in shortening the duration of inflammation.

The post hoc analysis employs the Tukey HSD/LSD test to ascertain variations in average values between two variables within the three experimental groups. Table 2 presents further difference tests of variables in TNF-α immunohistochemistry among groups. The comparison of Group A with Group C on days 7 and 14 revealed a significance level of p<0.05, indicating a significant difference between these two groups on both observation days. On the other hand, when examining research groups A and B, the significance values for days 7 and 14 were p>0.05. This value indicates no significant difference was observed between the two variables within experimental groups A and B on both observation days.

Discussions

Bone graft material serves a multifaceted role by aiding in reconstruction, stabilizing bone structures, and promoting osteogenesis to facilitate bone healing [11,12]. Utilizing bone grafts to replace lost or damaged bone structures resulting from trauma or periodontal disease is expected to enhance the wound-healing process and stimulate the formation of new bone [11,12]. In this current study, we investigated the impact of bone graft materials obtained from pearl oyster shells on TNF-α levels. Our findings suggest that this material can potentially expedite bone healing and regeneration by reducing TNF-α levels.

It has been known that the nacre found in pearl oyster shells and the mineral structure comprising bone share striking similarities despite variations in ingredient composition [13]. While human bones predominantly comprise calcium phosphate, pearl oyster shells consist mainly of calcium carbonate in the form of aragonite crystals [13,14]. Pearl oyster shells tend to have a relatively high calcium carbonate content, averaging 94.873 ± 0.04%, surpassing other types of shellfish [13]. This calcium carbonate content within seashells serves as a calcium source, which can be harnessed as material for synthesizing hydroxyapatite [13]. In the present study, we found that Pinctada maxima has therapeutic potential and can facilitate the healing of wounds. We found a reduction in the average TNF-α levels across all treatments on days 7 and 14, suggesting a decrease in inflammation. These findings align with a study by Darbois et al. (2021) that found that nacre can support bone apposition without triggering excessive inflammatory responses from the host [15].

Recently, there has been a growing interest in understanding the impact of hydroxyapatite on the inflammatory process [14-16]. For instance, Gani et al. (2022) conducted research involving a combination of chitosan gel and hydroxyapatite extracted from crab shells (Portunus pelagicus) [16]. Their findings demonstrated a significant enhancement in BMP2 levels, a protein associated with bone growth [16]. Similarly, in the study by Adam et al. (2022), golden sea cucumber (Stichopus hermanni) was investigated as a bone graft material [17]. Their research revealed increased osteoblast and osteocalcin expression in guinea pig femur bone defects, indicating that hydroxyapatite sourced from the golden sea cucumber could expedite the process of bone regeneration [17].

In the current study, significant differences emerge when comparing the mean levels of TNF-α among groups on both the 7th and 14th days. Specifically, there is a significant difference between the untreated group and the group that received Hydroxyapatite Pinctada maxima bone grafts combined with PRF. However, no significant difference is observed between the group that received Hydroxyapatite Pinctada maxima bone grafts alone and the group that re-

Table 2. Analysis of the LSD ratio between different study groups on days 7 and 14.

Observation	Variable between groups	p-value
7	Group A (negative control) VS Group B (HPM alone)	0.144
	Group A (negative control) VS Group C (HPM+PRF)	0.001*
	Group B (HPM alone) VS Group C (HPM+PRF)	0.219
14	Group A (negative control) VS Group B (HPM alone)	0.056
	Group A (negative control) VS Group C (HPM+PRF)	0.000*
	Group B (HPM alone) VS Group A (negative control)	0.726

*Post Hoc LSD; p<0.05 significant

ceived Hydroxyapatite Pinctada maxima bone grafts with PRF on both the 7th and 14th days. This suggests that using naturally sourced hydroxyapatite from pearl shells can reduce the inflammatory processes, consequently expediting bone regeneration. Furthermore, the incorporation of PRF enhances the therapeutic efficacy of the bone graft material. This result is consistent with previous studies, highlighting the crucial role of PRF in cell growth, proliferation, differentiation, and healing [18-20]. PRF is stored in platelets and released upon platelet activation, serving as a vital component in wound healing, tissue regeneration, and its hemostatic function [19,20]. The PRF fibrin network's natural polymerization process preserves the fibrin matrix's physiological architecture, further promoting the healing process [18,20]. Due to its ease of production, cost-effectiveness, and autologous nature, PRF has found successful applications in regenerative medicine [19].

While this study provides valuable insights into the effects of pearl oyster shell-derived bone grafts on TNF-α levels in patients with periodontal disease, the study also presents certain considerations. The modest sample size of male guinea pigs and the exclusive inclusion of this demographic in the animal model may restrict the generalizability of the findings to broader populations. Additionally, the study's focus on a relatively short observation period of 14 days limits the comprehensive understanding of the longer-term effects of the interventions. Furthermore, the study primarily examines the chemical and structural properties of HPM through analytical methods without directly assessing its clinical efficacy or effectiveness in promoting bone regeneration. Despite these limitations, the study contributes to our understanding of the therapeutic potential of natural bone grafts in periodontal therapy. It may inform the development of adjunctive therapies for periodontal disease management, shedding light on the broader connections between oral health and systemic inflammation.

Conclusion

Bone graft material derived from pearl oyster shells (Pinctada maxima) is characterized by its rich hydroxyapatite content, reducing inflammation duration and expediting bone healing. Integrating PRF into this bone graft material has demonstrated its efficacy in hastening bone regeneration. These findings serve as a valuable reference for developing advanced bone graft materials.

Authors' contribution

SO (Conceptualization, Data curation, Formal Analysis, Methodology, Validation, Supervision, Writing – review & editing)

NH (Conceptualization, Data curation, Formal Analysis, Funding acquisition, Investigation, Methodology, Project administration, Validation, Supervision, Writing – review & editing)

M (Resources, Software, Visualization, Writing – original draft)

DS (Data curation, Supervision, Validation, Writing – review & editing)

ASHY (Data curation, Validation, Writing – review & editing)

Conflict of interest

None to declare.

References

1. Annunziata M, Piccirillo A, Perillo F, Cecoro G, Nastri L, Guida L. Enamel matrix derivative and autogenous bone graft for periodontal regeneration of intrabony defects in humans: A systematic review and meta-analysis. Materials. 2019 Aug 19;12(16):2634.
2. Machado V, Botelho J, Neves J, Proença L, Delgado A, Mendes J. The prevalence of periodontal diseases in Portugal and correspondent digital awareness for the period 2004-2017: analysis of data from Global Burden of Disease and Google Trends. Rev Port Estomatol Med Dent Cir Maxilofac. 2020 Mar;61:10-6.
3. Miron RJ, Moraschini V, Fujioka-Kobayashi M, et al. Use of platelet-rich fibrin for the treatment of periodontal intrabony defects: A systematic review and meta-analysis. Clin Oral Investig. 2021:25;2461-2478.
4. Chan JK, Glass GE, Ersek A, et al. Low-dose TNF augments fracture healing in normal and osteoporotic bone by up-regulating the innate immune response. EMBO Mol. Med. 2015 May;7(5):547-61.
5. Coringa R, de Sousa EM, Botelho JN, et al. Bone substitute made from a Brazilian oyster shell functions as a fast stimulator for bone-forming cells in an animal model. Plos one. 2018 Jun 5;13(6):e0198697.
6. Chandha MH, Mappangara S, Achmad H, Oktawati S, Buddin M, Tetan-El D, Salam F, Halik H. Utilization Effectivity Of Pearl Oyster Shell (Pinctada Maxima) As Industrial Waste In Pangkep To Osteogenesis Bone Graft To Cavia Porcellus Femur. J. Pharm. Negat. 2023 Jan 1:218-25.
7. Jo YY, Kweon H, Kim DW, Baek K, Kim MK, Kim SG, Chae WS, Choi JY, Rotaru H. Bone regeneration is associated with the concentration of tumour necrosis factor-α induced by sericin released from a silk mat. Sci Rep. 2017 Nov 14;7(1):15589.
8. Salim I, Kamadjaja MJ, Dahlan A. Tumor necrosis factor-α and osterix expression after the transplantation of a hydroxyapatite scaffold from crab shell (Portunus pelagicus) in the post-extraction socket of Cavia cobaya. Dent J. 2022;55(1):26-32.
9. Hutton DL, Kondragunta R, Moore EM, Hung BP, Jia X, Grayson WL. Tumor necrosis factor improves vascularization in osteogenic grafts engineered with human adipose-derived stem/stromal cells. PLoS One. 2014 Sep 23;9(9):e107199.
10. Humidat AK, Kamadjaja DB, Bianto C, Rasyida AZ, Harijadi A. Effect of freeze-dried bovine bone xenograft on tumor necrosis factor-alpha secretion in human peripheral blood mononuclear cells. Asian Jr of Microbiol Biotech Env Sc. 2018;20:S88-92.
11. Reynolds MA, Aichelmann-Reidy ME, Branch-Mays GL. Regeneration of periodontal tissue: bone replacement grafts. Dent Clin North Am. 2010 Jan;54(1):55-71.
12. Stavropoulos A, Bertl K, Spineli LM, Sculean A, Cortellini P, Tonetti M. Medium- and long-term clinical benefits of periodontal regenerative/reconstructive procedures in intrabony defects: Systematic review and network meta-analysis of randomized controlled clinical studies. J Clin Periodontol. 2021 Mar;48(3):410-30.
13. Zhang G, Brion A, Willemin AS, et al. Nacre, a natural, multi-use, and timely biomaterial for bone graft substitution. J Biomed Mater Res A. 2017 Feb;105(2):662-71.
14. Shaikh MS, Zafar MS, Alnazzawi A, Javed F. Nanocrystalline hydroxyapatite in regeneration of periodontal intrabony defects: A systematic review and meta-analysis. Ann Anat. 2022 Feb 1;240:151877.
15. Kün-Darbois JD, Libouban H, Camprasse G, Camprasse S, Chappard D. In vivo osseointegration and erosion of nacre screws in an animal model. J Biomed Mater Res B Appl Biomater. 2021 Jun;109(6):780-8.
16. Gani A, Yulianty R, Supiaty S, et al. Effectiveness of combination of chitosan gel and hydroxyapatite from crabs shells (Portunus pelagicus) waste as bonegraft on periodontal network regeneration through IL-1 and BMP-2 analysis. Int J Biomater. 2022 Mar 20;2022.
17. Adam M, Achmad H, Nasir M, Putri SW, Azizah A, Satya DE. Stimulation

of osteoblast and osteocalcin in the bone regeneration by giving bonegraft golden sea cucumber. J Int Dent Med Res. 2022;15(1):140-7.
18. Rhael Ali M, Rasool Hammoodi SA. Assessment of the Impact of Platelets-Rich Fibrin on Healing Process after Teeth Extraction. Indian J Public Health Res Dev. 2019 Feb 1;10(2).
19. Pavlovic V, Ciric M, Jovanovic V, Trandafilovic M, Stojanovic P. Platelet-rich fibrin: Basics of biological actions and protocol modifications. Open Med. 2021 Mar 22;16(1):446-54.
20. Goel A, Windsor LJ, Gregory RL, Blanchard SB, Hamada Y. Effects of platelet-rich fibrin on human gingival and periodontal ligament fibroblast proliferation from chronic periodontitis versus periodontally healthy subjects. Clin Exp Dent. 2021 Aug;7(4):436-42.